

Light trapping in thin silicon solar cells: A review on fundamentals and technologies

Rebecca Saive 

MESA+ Institute for Nanotechnology,
 Inorganic Materials Science, University of
 Twente, Enschede, The Netherlands

Correspondence

Rebecca Saive, MESA+ Institute for
 Nanotechnology, Inorganic Materials Science,
 University of Twente, Enschede 7522 NB, The
 Netherlands.
 Email: r.saive@utwente.nl

Abstract

Thin, flexible, and efficient silicon solar cells would revolutionize the photovoltaic market and open up new opportunities for PV integration. However, as an indirect semiconductor, silicon exhibits weak absorption for infrared photons and the efficient absorption of the full above bandgap solar spectrum requires careful photon management. This review paper provides an overview on the fundamental physics of light trapping and explains known theoretical limits. Technologies that have been developed to improve light trapping will be discussed, and limitations will be addressed.

KEY WORDS

absorption, light management, light trapping, photonics, physics, silicon photovoltaics, solar cells, solar energy

1 | INTRODUCTION

Forty years after Eli Yablonovitch submitted his seminal work on the statistics of light trapping in silicon,¹ the topic has remained on the forefront of solar cell research due to the prevalence of silicon in the photovoltaic (PV) industry since its beginnings in the 1970s.^{2,3} Despite the rise of a plethora of alternative technologies, more than 90% of newly installed PV plants are still based on silicon.³ The reasons for this are multifaceted; certainly, silicon PV is the most mature and reliable technology with the first modern solar cell ever made dating back to 1954.⁴ Coincidentally, silicon does not only encompass excellent material properties—with respect to both performance and processability—it also happens to be the second most abundant material in earth's crust.⁵ The cost of silicon has seen some volatility in the past due to rapid demand increases with limited manufacturing capabilities,⁶ while the silicon wafer contributes an average of 14% to total module production costs.⁷ Therefore, it is of economic interest to reduce the amount of silicon used in a PV cell by reducing the absorber thickness.⁸ It will be further detailed below that thickness reductions can also lead to efficiency enhancements and to mechanical flexibility. However, crystalline silicon is an indirect semiconductor and therefore exhibits poor absorption for low-energy photons.⁹ To

ensure complete absorption of the above bandgap solar spectrum, the optical path length of light within the silicon must be increased. Strategies that increase the optical path length with the goal to mitigate photon escape are referred to as light-trapping methods.¹⁰

In this paper, the fundamentals of light trapping in crystalline silicon will be discussed and a review is presented on existing light-trapping strategies. First, the optical properties of silicon and the benefits of thin silicon solar cells will be addressed. Subsequently, known theoretical concepts will be derived and discussed. The fifth part of the paper presents examples of existing light-trapping strategies. The sixth part discusses two practical issues arising from advanced light-trapping technologies: parasitic absorption and surface recombination. In summary, this review provides a comprehensive overview on the topic of light-trapping in silicon with the goal to facilitate the development and benchmarking of emerging strategies.

2 | OPTICAL PROPERTIES OF SILICON

Silicon is an indirect semiconductor with a bandgap of 1.124 eV at room temperature,¹¹ which corresponds to a vacuum wavelength of 1103 nm. The band structure of silicon as determined by

This is an open access article under the terms of the Creative Commons Attribution License, which permits use, distribution and reproduction in any medium, provided the original work is properly cited.

© 2021 The Author. Progress in Photovoltaics: Research and Applications published by John Wiley & Sons Ltd.

Chelikowsky and Cohen is presented in Figure 1A.¹² The band structure relates the electron momentum within the crystal, expressed by its wave vector k , with the energy of the electron. The relation depends on the direction of the momentum relative to the crystal directions. The crystal directions in reciprocal or momentum space are displayed on the x axis in Figure 1A. Regions of the band diagram in which no possible k vector exist for a certain energy are called an energetic bandgap.¹³ The states above the bandgap belong to the conduction band, and the states below the bandgap belong to the valence band. The numerical value of the bandgap is defined as

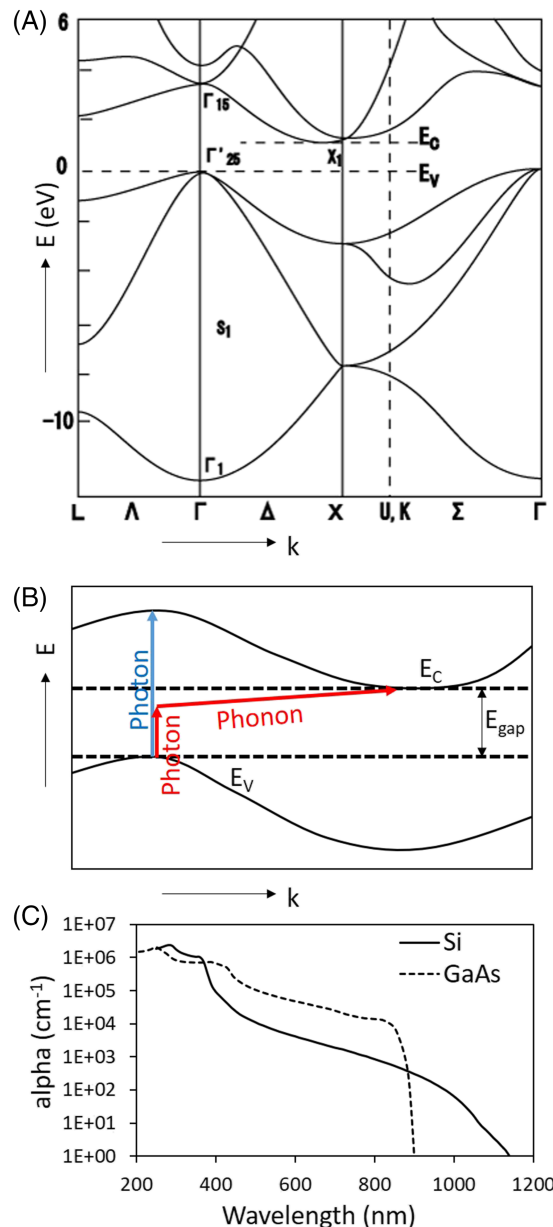


FIGURE 1 (A) Band diagram of silicon according to Chelikowsky and Cohen.¹² (B) Schematics of direct and phonon-assisted optical transitions. (C) Wavelength-dependent absorption coefficient of silicon and GaAs. Data from Green and Aspnes and Studna^{9,14}

the energetic difference between the highest point of the valence band and the lowest point of the conduction band.¹³ Through absorption of photons and phonons (i.e., crystal lattice vibrations), electrons can be excited from the valence into the conduction band. This process is called an interband transition. Photons barely carry momentum, while phonons barely carry energy. For an electron to significantly change its energy, it needs to absorb a photon, and to change its momentum, it needs to absorb a phonon. Silicon is an indirect semiconductor, which means that the maximum of the valence band and the minimum of the conduction band occur for different k vectors. Accordingly, for an interband transition to occur, either the photon energy has to be significantly larger than E_{gap} as shown by the blue arrow in Figure 1B or the transition has to be performed by simultaneous absorption of a photon and a phonon¹³ as shown by the red arrows in Figure 1B. As the latter process involves three particles rather than only two, it is less likely than a direct transition. Therefore, indirect semiconductors such as silicon absorb less strongly for photon energies right above their bandgap. Figure 1C shows the wavelength-dependent absorption coefficient of silicon⁹ and GaAs.¹⁴ The direct bandgap in GaAs leads to a steep onset of its absorption coefficient near the bandgap, whereas the absorption coefficient of silicon increases slowly with decreasing photon wavelength. Thus, for the absorption of the full above bandgap solar spectrum, GaAs solar cells can be made thin, typically in the order of a few hundred nanometers to a couple of micrometers,¹⁵ while silicon solar cells have to be significantly thicker, typically in the range of 100–500 μm .¹⁶

3 | PROPERTIES OF THIN SILICON

While the economic benefits of decreasing material usage were briefly discussed in Section 1, this section focusses on the physical properties of thin silicon. The section is divided into the mechanical and electrical properties of thin silicon.

3.1 | Mechanical properties

When thinning a material, the obvious advantage that comes to mind is a reduction in weight. However, silicon solar cells have to be carefully encapsulated and packaged to avoid degradation and mechanical failure such as cracking. The encapsulation is usually performed with several hundreds of micrometers of EVA and a few millimeter-thick glass.¹⁷ Compared to the approximately 100 μm of silicon, the weight of the EVA and glass dominate the overall module weight. Furthermore, when thinning silicon from a few 100 μm to 50 μm , silicon becomes brittle and fragile and handling such thin wafers becomes increasingly difficult.¹⁶ However, when decreasing thickness even further, eventually silicon stops being brittle and instead starts becoming flexible.^{18,19} Figure 2 shows pictures of silicon with a thickness of 10 μm being either bent²⁰ or cut with scissors.²¹ Therefore, a high performing silicon solar cell with thickness of 10 μm or less would be

highly desirable for mechanical reasons and would allow easy integration of silicon solar cells with any surfaces. Very thin and flexible high efficiency solar cells have been demonstrated based on GaAs.^{22,23} Contrary to silicon, GaAs is a direct bandgap semiconductor, and hence, less than a couple micrometer thickness is sufficient for complete solar spectrum absorption. While very desirable for economic and ease of use reasons, obtaining thin, flexible, and yet highly efficient silicon solar cells is only possible through very effective light trapping. Yet first flexible crystalline solar cells have been demonstrated^{19,24}; for example, Xue et al. reported an efficiency of 12.3% with only 2.7-μm silicon thickness.²⁵

3.2 | Electrical properties

A solar cell is an optoelectronic device, and while efficient photon collection is crucial, optimizing the electrical properties is equally important. The thickness influences the electrical properties in many different ways. In this section, the influence of thickness on short-circuit current density, open-circuit voltage, and fill factor will be discussed. The short-circuit current density j_{sc} of a solar cell is determined by the external quantum efficiency $EQE(\lambda)$ and the solar irradiance flux $\Phi(\lambda)$ via

$$j_{sc} = \int_0^{\lambda_{gap}} EQE(\lambda) \Phi(\lambda) d\lambda$$

where λ_{gap} is the wavelength that corresponds to the bandgap energy. The external quantum efficiency describes how many electron hole pairs are created out of incoming photons with a specific wavelength and can in turn be described by the absorption within the absorber material $A(\lambda)$ and by the charge carrier collection efficiency, also called internal quantum efficiency $IQE(\lambda)$:

$$EQE(\lambda) = A(\lambda) IQE(\lambda)$$

Evidently, the absorption is the main topic of this paper and will be discussed further below. The carrier collection efficiency depends on the diffusion length of the charge carriers and on where charge carriers are generated. In essence, charge carriers need to be able to diffuse to the contacts and must not recombine through any other channel before. For high-quality crystalline silicon, almost 100%

internal quantum efficiency can be achieved.^{26,27} Hence, for a silicon solar cell, j_{sc} is mainly determined by the absorption.

The maximum open-circuit voltage in a solar cell is determined by the difference between the quasi-Fermi level of electrons and the quasi-Fermi level of holes. This quasi-Fermi-level splitting increases with increased photocharge carrier generation and decreases with increasing recombination. Therefore, to increase the open-circuit voltage, the short-circuit current should be increased and the dark current of the cell should be decreased. The open-circuit voltage V_{OC} can be expressed by the short-circuit current density j_{sc} and the dark current density j_0 of a solar cell via²⁸

$$V_{OC} = \frac{k_B T_{cell}}{q} \ln \left(\frac{j_{sc}}{j_0} + 1 \right)$$

where k_B is the Boltzmann constant, T_{cell} is the temperature of the solar cell, and q is the charge of an electron. A rigorous derivation of the open-circuit voltage can, for example, be found in Würfel and Würfel.²⁹ The open-circuit voltage has been shown to improve with decreasing thickness of silicon (heterojunction) solar cells.³⁰⁻³³ Thinning the wafer leads to decreased charge carrier recombination in the bulk³⁰ and to increased charge carrier concentration—as long as the photocharge carrier generation remains constant and excellent surface passivation is provided—which in turn leads to increased open-circuit voltage.^{34,35} Vice versa, if the recombination and dark current remain the same and $j_{sc}/j_0 \gg 1$, then the difference in open-circuit voltage ΔV_{OC} depends logarithmically on the factor y with which the short-circuit current density changes:

$$\Delta V_{OC} = \frac{k_B T_{cell}}{q} \ln(y)$$

Consequently, any improvements on the short-circuit current will also improve the open-circuit voltage.

The fill factor of a solar cell is related to the open-circuit voltage³⁶ and to the series and shunt resistances.³⁷ A thinner cell can be beneficial for the fill factor due to the higher open-circuit voltage,³⁶ but a strong correlation is not always observed.³³ Thinning the wafer thickness decreases the vertical series resistance but increases the lateral series resistance.

All in all, thin silicon solar cells are desirable for several reasons as long as full light absorption can be achieved.

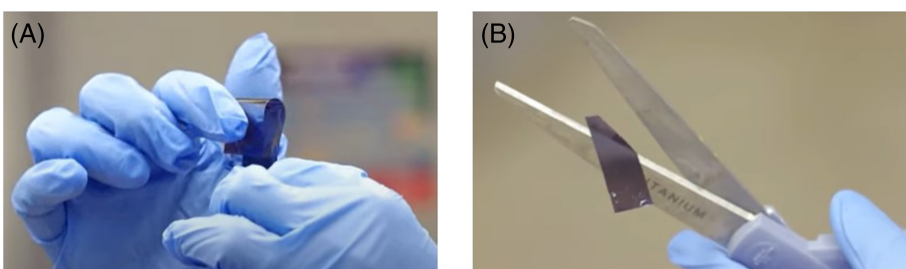


FIGURE 2 (A) Bending and (B) scissor cutting of 10-μm-thick silicon. From Cui^{20,21}

4 | THE FUNDAMENTALS OF LIGHT TRAPPING

In this section, the fundamentals of light trapping will be discussed. First, the concept of path length enhancement will be introduced, then the Lambertian limit, also called Yablonovitch or $4n^2$ limit, will be explained. It will be shown how the local optical density of states (LDOS) relates to this limit and how through manipulation of the LDOS the Lambertian limit can be beaten.

4.1 | Path length enhancement

The Lambert–Beer law states that the extinction of light within absorptive media is described by

$$I(x, \lambda) = I_0 e^{-\alpha(\lambda)x}$$

where I is the intensity of light having traveled a distance x and I_0 is the intensity at $x = 0$. α is the absorption coefficient, which is connected to the imaginary part of the refractive index n_k of the material and to the vacuum wavelength λ by $\alpha = 4\pi n_k / \lambda$. Hence, the amount of light that is absorbed in a medium depends on the distance x traveled through the medium, also called the path length, and on the absorption coefficient α , which in turn depends on the wavelength as shown in Figure 1C. Figure 3 provides an understanding on how long of a distance light with a spectral distribution according to the standard AM 1.5 spectrum has to travel through silicon in order to be fully absorbed. The graph presents the corresponding short-circuit current density that is lost due to transmission through the silicon dependent on the thickness calculated via

$$j_{sc\ loss}(t) = j_{sc\ max} - j_{sc} = \int_0^{t_{gap}} \Phi(\lambda) d\lambda - \int_0^{t_{gap}} A(\lambda, t) \Phi(\lambda) d\lambda$$

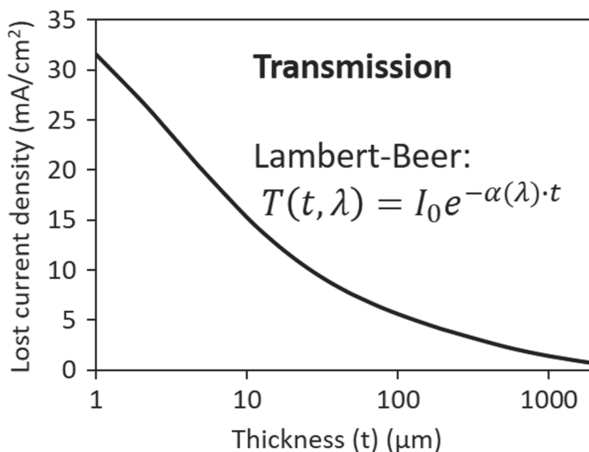


FIGURE 3 Equivalent short-circuit current density lost due to transmission depending on the thickness of silicon calculated with the Lambert–Beer law for the AM 1.5 spectrum

For the thickness and wavelength-dependent absorption $A(\lambda, t)$, it was assumed that no other losses (such as reflection) occur, and hence, the absorption is equal to 1 minus transmission:

$$A(\lambda, t) = 1 - T(\lambda, t)$$

The maximum current $j_{sc\ max}$ that could be generated from the AM 1.5 spectrum with a material with 1.12-eV bandgap, if all above bandgap photons were absorbed, is $44 \text{ mA}/\text{cm}^2$.

Figure 3 shows that to almost fully absorb the AM 1.5 spectrum, 1 mm of silicon would have to be used, which is significantly thicker than even conventional solar cells, currently ranging at around 180- μm thickness. Increasing the absorption while maintaining or even decreasing the silicon thickness requires light-trapping strategies that enhance the path length x of the light. One way to avoid the escape of light on the rear is by placing a mirror, which immediately doubles the path length and is done in almost all monofacial solar cells. But even doubling of the path length is not enough to achieve loss-free absorption, and rather, it is desirable to have light traveling under an angle to the surface. This can, for example, be achieved by texturing the front and rear surface as will be explained further below. In the next section, the theoretical limits and alternative ways to look at path length enhancement will be discussed. Guidelines on how to measure the path length enhancement can be found in this review paper by Mokkapati and Catchpole.³⁸

4.2 | Lambertian limit

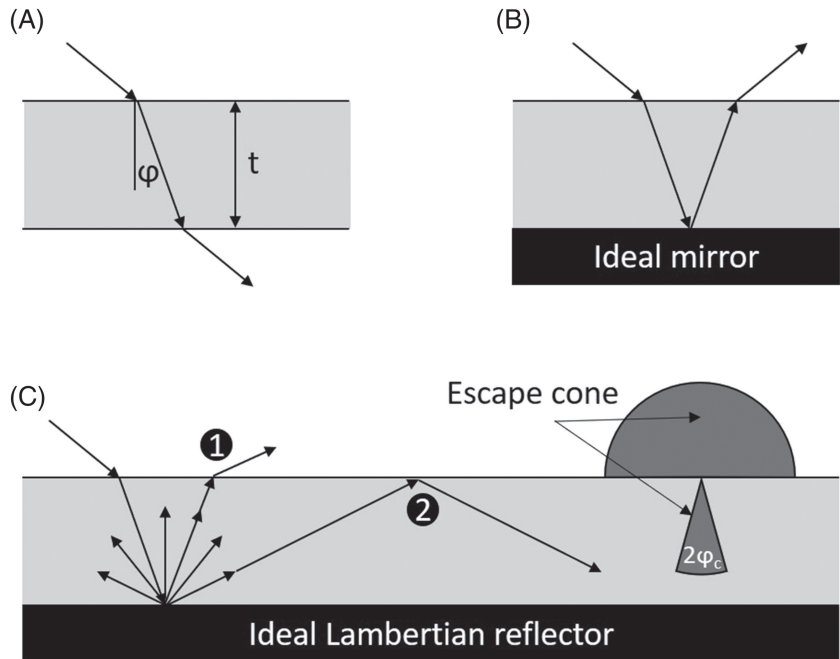
The Lambertian limit is also referred to as the $4n^2$ limit or as the Yablonovitch limit acknowledging its first publication in 1982.¹ There are different ways of deriving this limit in a ray optical picture. As the original derivation by Yablonovitch is widely available in literature (e.g., Fonash¹⁰), here, a different derivation is presented, which is only briefly mentioned by Yablonovitch as the geometric series approach.¹

Let us imagine a slab of silicon in air—thick enough so that wave optical effects do not occur—and light incident with energy close to the band edge, such that we obtain weakly absorbing conditions. In the case of a smooth front and rear surface (Figure 4A), the light ray will enter the material under an angle φ to the surface normal, whereas φ depends on the incoming angle and the refractive index according to Snell's law. The absorption path length x through the silicon will be

$$x = t/\cos(\varphi)$$

where t is the thickness of the slab. For weakly absorbing conditions, most of the light will exit the slab at the rear as depicted in Figure 4A. Escape on the rear can easily be avoided by placing a mirror on the rear as shown in Figure 4B. An ideal mirror enhances the path length by a factor of 2, but for a weakly absorbing medium, there will still be escape on the top surface. If instead of an ideal specular mirror, we use an ideal Lambertian reflector, the light will be randomized in its

FIGURE 4 Schematic of light with energy close to the bandgap passing through a thin silicon slab in air (A) without any light trapping, (B) with ideal specular mirror, and (C) with ideal Lambertian reflector on the rear side. In (C), the escape cone of $\alpha_c = 16.30^\circ$ within the silicon and the air escape/acceptance cone that corresponds to the full hemisphere are shown



direction upon reflection on the rear. The Lambertian light-trapping limit assumes perfect randomization of the light within the silicon, whereas it does not matter how this randomization is achieved. In the following, we are discussing the case of an ideal Lambertian rear reflector, but a textured front surface could achieve the same randomization. Depending on its angle, light reaching the front surface will either escape (Figure 4C, arrow 1) or encounter total internal reflection (TIR) (Figure 4C, arrow 2). The critical angle φ_c at which the transition between escape and TIR occurs is given by

$$\varphi_c = \arcsin(1/n)$$

And with small-angle approximation:

$$\varphi_c \approx 1/n$$

This defines a three-dimensional cone within which light can escape as shown in Figure 4C. For silicon at a wavelength of 1000 nm, the refractive index amounts to 3.572,⁹ and hence, $\varphi_c = 16.30^\circ$. Note that on the air side, light can be accepted from the full hemisphere and will also escape into angles within the full hemisphere due to reciprocity. Let us now derive the probability for randomized light to escape through the escape cone. To calculate this probability, we need to divide the number of rays within the escape cone by the total number of rays. Due to the perfect randomization, we can assume an isotropic distribution of rays, and hence, the number of rays within the escape cone is proportional to the solid angle of the sphere element defined by $2\varphi_c$. In small-angle approximation, this solid angle becomes

$$S_{\alpha_c} = \pi\varphi_c^2 = \frac{\pi}{n^2}$$

The total number of rays is proportional to the surface of the full hemisphere. This leads to a probability of escape P_e :

$$P_e = \frac{\pi}{n^2/2\pi} = \frac{1}{2n^2}$$

From this result, there are two different strategies to derive the intensity within the silicon slab: (1) a simple detailed balance consideration and (2) summing up over all possible reflections via a geometric series. In both cases, it is assumed that no photons are lost other than through escape within the front surface escape cone. In other words, no photons are absorbed in the bulk or at the surfaces. In this case, detailed balance dictates that the number of incoming photons $\#_{inc}$ is equal to the number of escaping photons $\#_{esc}$. As $P_e = \frac{1}{2n^2}$, and the number of photons $\#_{S1}$ reaching the front surface must be $2n^2\#_{inc}$ in order to ensure $\#_{esc} = P_e\#_{S1} = \#_{inc}$. The same result is reached when adding up all reflections that occur at the front surface:

$$\begin{aligned} \#_{S1}/\#_{inc} &= (1 - P_e) + (1 - P_e)^2 + (1 - P_e)^3 + \dots + (1 - P_e)^n \\ &= \frac{1}{1 - (1 - 1/2n^2)} = 2n^2 \end{aligned}$$

Hence, we derive that the intensity of rays within the silicon slab going towards the upper hemisphere is $2n^2$ greater than the intensity of incoming photons. For isotropy reasons, the same is true for the intensity of photons going towards the bottom surface. Therefore, in total, we have increased the number of rays by a factor of $4n^2$ as compared to the incoming number of rays, and these rays are isotopically

distributed over the whole solid angle within the silicon. Again, from here, there are multiple ways to determine the effective path length enhancement. One way is to determine the absorption within a volume element as described by Yablonovitch and as schematically presented in Figure 5A. First, we define B as the internal intensity per unit internal solid angle, which is an isotropic function with constant value of

$$B = \frac{4n^2}{4\pi} = \frac{n^2}{\pi}$$

Absorption A within a volume element $dV = tdA_i$ is then given by

$$A = 2at \int_0^{2\pi} d\theta \int_0^{\pi/2} B \cos\varphi d\varphi = 4\pi at B = 4n^2 at$$

This equation yields the famous $4n^2$ absorption enhancement. Again, it is assuming weak absorption, so no change in intensity across the thickness of the silicon slab and perfect light randomization, that is, isotropic light conditions within the slab. For a more general derivation of the Lambertian limit that does not require weak absorption, the author refers to work by Green.³⁹

An alternative way to arrive at the $4n^2$ absorption enhancement is depicted in Figure 5B. One can assume each point of the surface to reflect light in an ideal Lambertian way, that is, distributed over the solid angle of a hemisphere with intensity dropping with $\cos(\varphi)$. At the same time, each reflected ray will have a path length of $t/\cos(\varphi)$. Therefore, the average length \bar{t} of a ray weighted with its intensity amounts to the slab thickness t :

$$\bar{t} = \cos(\varphi) \cdot t / \cos(\varphi) = t$$

In Figure 5B, there are three different rays shown, which despite their different length, all have the same intensity weighted length \bar{t} . There are $4n^2 \#_{inc}$ rays inside the slab as derived above, and hence, the path length enhancement amounts to $4n^2$.

In this section, the Lambertian light-trapping limit was derived from a ray optical perspective, with a slightly different but yet equivalent path to the original work by Yablonovitch.¹ In the following, this result will be connected with statistical mechanics, and it will be

shown that the Lambertian limit is not actually a hard limit in the thermodynamic sense but can be overcome through design of the optical environment.

4.3 | Statistics and density of states

In the following section, we will derive the Lambertian limit from a statistics point of view. Again, the emphasis is on motivating the derivation conceptionally, while approaching the topic from a slightly different angle than other literature sources. First, let us take a look at the LDOS in a medium, which shall be homogeneous and isotropic throughout the section. The LDOS is defined as the number of existing states per unit volume at a certain energy and can be derived from the dispersion relation, that is, from the relation between momentum and energy. The dispersion relation is shown in Figure 6 for light in vacuum (blue curve) and light in a homogenous, isotropic, and nondispersive medium with refractive index n (red curve). The LDOS at a certain energy is derived by summing all states in k space that lie at this specific energy. To visualize this concept, the states that are at constant energy in a two-dimensional system are drawn as a blue (light in vacuum) and red (light in a medium) circle. Therefore, in two dimensions, the LDOS scales with the circumference of a circle with radius $|\vec{k}|$, that is, the length of the wave vector. In a medium with refractive index n , $|\vec{k}| = n|\vec{k}_0|$, where $|\vec{k}_0|$ is the wave vector in vacuum. In three dimensions, states of equal energy are described by the surface of a sphere $S_{sp} = 4\pi|\vec{k}|^2$ with radius corresponding to the length of the wave vector. Therefore, in a medium with refractive index n , the surface of the sphere is proportional to n^2 .

This means that in a 3D homogenous, isotropic, and non-dispersive medium with refractive index n , the LDOS is n^2 higher than in vacuum. Now, we imagine the (isotropic and homogenous) silicon slab sitting in vacuum and within isotropic irradiance. Furthermore, we consider an ergodic system, that is, a system in which all states with the same energy are equally likely to be populated. In this case, the available states within and outside of the silicon slab will be populated according to Bose–Einstein distribution statistics. As the LDOS within the silicon is n^2 higher than outside, we will have an n^2 higher light intensity within the silicon. Once we place a mirror, the system is no longer ergodic, as there is no exchange between all states possible anymore. In this case, we can use the same arguments as explained in

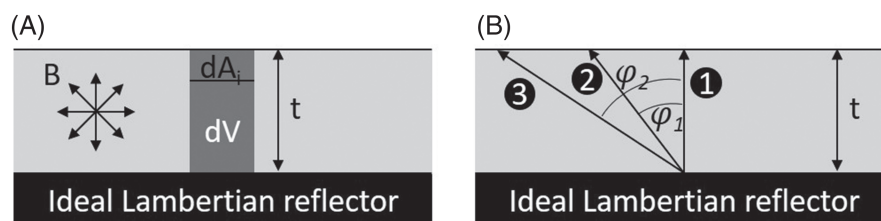


FIGURE 5 (A) Schematic of how absorption enhancement can be calculated in a weakly absorbing slab with isotropic internal irradiance. (B) Schematic on how absorption enhancement can be calculated by assuming that all points on the surface reflect in Lambertian way; that is, rays are reflected towards all directions with $\cos(\varphi)$ intensity distribution

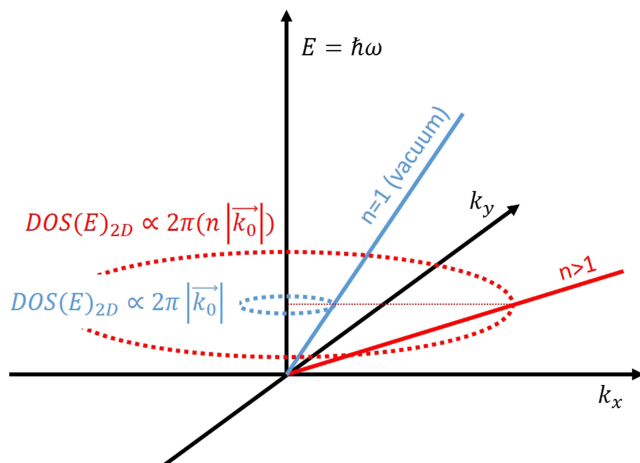


FIGURE 6 Dispersion relation for light in vacuum (blue) and in a homogenous and isotropic medium (red). The blue and red circle depict the two-dimensional LDOS for vacuum and medium with refractive index n , both at the same energy

the previous section. All in all, we have seen in this section that the Lambertian limit can also be derived from a statistics point of view, whereas the LDOS—which in a homogenous and isotropic medium scales with n^2 —determines the ratio of intensity enhancement. Therefore, designing the LDOS is a possible route to improve light trapping.

Concretely, there are two different routes to achieve this goal: (1) decreasing the LDOS outside of the silicon or (2) increasing the LDOS within the silicon. We will see below how such tasks can be performed, for example, with gratings or photonic crystals. It is important to note that, without such alterations of the LDOS, the $4n^2$ limit cannot be overcome³⁸! Naturally, LDOS modification also exhibits fundamental limits. The smallest LDOS possible in air would mean that light can only escape from the silicon into air under one specific angle. Due to reciprocity, this means that light would also only be allowed to enter from one certain direction. Therefore, strategies that decrease the air LDOS inherently also decrease the light acceptance angle³⁸ and hence can never work properly without sun tracking or under diffuse light conditions.^{40,41} This principle, also known as étendue conservation,^{42,43} manifests, for example, in the comparison between monofacial and bifacial solar cells: monofacial solar cells accept light only from the front and use a rear mirror for improved light trapping. Bifacial solar cells can accept light from front and rear, thereby providing great benefits for converting diffused and albedo reflected light, but performing slightly less good under direct light conditions due to the less good light trapping.⁴⁴ Researchers that claim to exceed the Lambertian limit with strategies based on geometrical optics⁴⁵ should carefully check the acceptance angle and their calculation of the Lambertian reference.

On a side note, reducing the air LDOS also reduces radiative recombination. In solar cells in which this is the dominant recombination mechanism, the dark current decreases, and therefore, the open-circuit voltage increases^{41,46–48} as also explained in Section 3.2.

5 | LIGHT-TRAPPING TECHNOLOGIES

This section presents an overview of different light-trapping methods and technologies that have been used in production or have otherwise been presented in literature.

5.1 | Pyramids

Pyramidal textures are the most common method to enhance the path length in silicon by randomizing the light direction. Their success is based on two major reasons: (1) industrial-scale texturing is feasible using anisotropic alkaline etching⁴⁹ and (2) close to perfect randomization can be achieved with pyramidal textures.⁵⁰

Figure 7A shows a scanning electron microscopy image of a silicon heterojunction solar cell with random pyramid texture captured under 45° viewing angle. In Figure 7B, the cross section of the same solar cell as in Figure 7A is shown. The surface profile was obtained via atomic force microscopy on different areas of the solar cell. Note that the bulk of the solar cell has a different scale bar than the surface to facilitate presentation. More information on this particular cell can be found in Russell et al.⁵¹ The influence of texture on the light path is explained by black arrows. An incoming ray can be either reflected (ray 1) or transmitted (ray 2) on the surface with a probability depending on its incident angle and on the interface properties. If a ray is reflected, the texture makes it likely that the reflected ray obtains another chance to enter the solar cell and subsequently be absorbed. Therefore, a front texture also improves antireflection properties.⁵² Ray 2 enters the solar cell under an angle that is dependent on the incident angle, on the surface normal, and on the refractive index. A textured surface exhibits a large distribution of surface normal across the surface, and so even light with constant incident angle will enter the solar cell under a wide distribution of angles. Thereby, the textured front surface randomizes the light direction inside the solar cell and increases the path length. For high-energy photons, this path length enhancement might be sufficient to ensure full absorption. However, infrared photons will most likely be transmitted to the rear interface where they often encounter another textured interface with rear mirror. The rear texture randomizes the light even further.⁵³ A combination of random front and rear texture has shown to provide close to ideal Lambertian properties.^{50,54,55}

A variety of different designs have been proposed based on the pyramid principle. Such designs can either be of random^{54,55} or of periodic^{56,57} nature and can employ either upright or inverted pyramids.^{24,56,58} A prominent example for inverted pyramids is the passivated emitter, rear locally diffused (PERL) cell that marked a new efficiency record in 1999.⁵⁹ Interestingly, it has been shown that random pyramids perform better than periodic arrays as they offer closer to Lambertian properties.^{54,55} Another variant of the inclined surface approach, which can also be fabricated with anisotropic etching, is triangular cross-sectional grooves.^{45,60}

The performance of such structures with respect to anti-reflection and light-trapping properties has been extensively

discussed in literature both in experimental^{53,57,61,62} and in computational^{52,54,55,63–66} studies. The referenced studies show several examples of pyramidal light-trapping structures. A comprehensive list of all literature references on this topic lies beyond the scope of this paper.

To summarize, random pyramids can provide Lambertian light trapping, which is the optimum light trapping achievable without manipulating the LDOS within or outside of the silicon. Commercial silicon solar cells employ random pyramids and so does the current world record silicon solar cell made by Kaneka with an efficiency of 26.7% and a thickness of 165 μm .⁶⁷ In addition to its excellent surface passivation and therefore high open-circuit voltage, this solar cell also features interdigitated back contacts (IBCs) avoiding front contact losses inherent to most other types of solar cells. This shows that for optimal light management, not only light trapping but also avoiding reflection and parasitic absorption is crucial.^{27,68}

If the thickness of the silicon absorber is reduced to only a few micrometers and is therefore similar to the pyramid size, (random) pyramids are no longer viable as Lambertian reflectors. The following sections will present light-trapping strategies that also work with very thin silicon. Note that most of these strategies rely on LDOS manipulation within or outside of the silicon and therefore have either limited acceptance angle or limited wavelength bandwidth.

5.2 | Gratings and photonic crystals

In this chapter, we will discuss light-trapping strategies based on periodic structures with periodicity being in the same order of magnitude as the wavelengths contained are the solar spectrum. Contrary to the micrometer-sized pyramids introduced in the previous chapter, a ray optical treatment is not possible for such structures. The mathematical description requires to use wave optical physics as dictated by Maxwell's equations.⁶⁹ In this section, nanostructures with periodic features will be discussed. Depending on the community and framework, such structures are referred to either as gratings or as photonic crystals. Because the term photonic crystal implies a periodic structure, we will use this term in the following. However, many of the literature examples that are cited refer to their structures as gratings.^{56,70,71}

A photonic crystal is a material with periodic modulation of the refractive index⁶⁹ resulting in an energetic band structure in reciprocal space equivalent to the electronic band structure in crystalline solids.⁷³ Similar to semiconductors, photonic crystals feature energetic bandgaps in which propagation of light is prohibited due to the absence of allowed states.⁷³ The dispersion relation or also called band diagram of a one-dimensional photonic crystal with reciprocal lattice constant g is shown in Figure 8A and compared with light in free space.⁶⁹ From such a (photonic) band structure, the LDOS can be derived as explained in Figure 6. A sketch of a possible LDOS of a

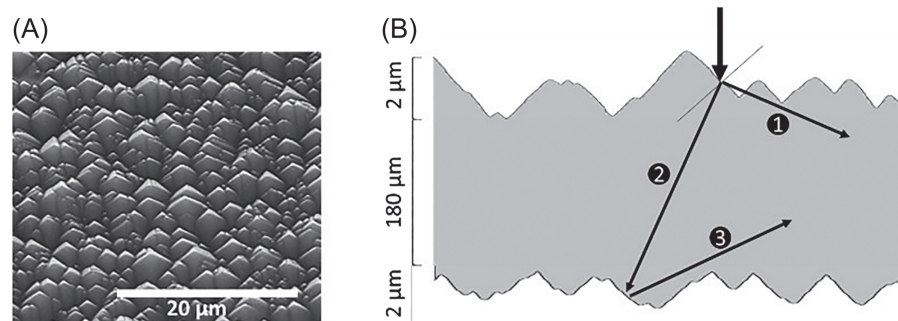


FIGURE 7 (A) Scanning electron microscopy (SEM) image of a textured silicon solar cell captured under 45° viewing angle. (B) Schematic of the three different ways in which pyramids randomize light: (1) reflecting on textured front, (2) transmission through textured front, and (3) reflection on textured rear. The texture in (b) corresponds to an atomic force microscopy profile of the solar cell shown in (a), which is described in more detail by Russell et al.⁵¹

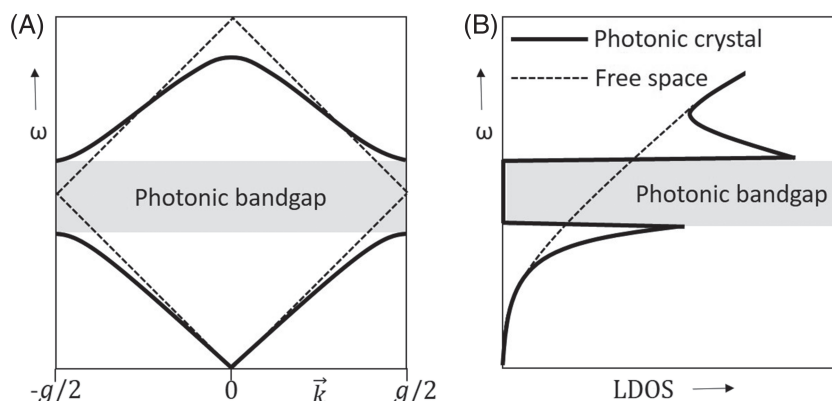


FIGURE 8 (A) Band diagram of a one-dimensional photonic crystal (bold line) and light in free space (dashed line).⁶⁹ (B) Sketch of the LDOS in a photonic crystal (bold line) and free space (dashed line)⁷²

photonic crystal compared to the LDOS in free space is shown in Figure 8B.⁷² Within the energetic bandgap area, the LDOS disappears; no propagation of light with the respective frequencies is allowed. Consequently, light incident on a photonic crystal within this frequency regime is perfectly reflected. The bandgap usually corresponds to a narrow frequency regime, and therefore, the observed reflection has a specific color. Furthermore, the frequency regime depends on the propagation direction, that is, a photonic crystal observed from different angles will appear in different colors. We can observe such color effects in nature, prominent examples are opals, butterfly wings, and bird feathers. Indeed, the origin of these natural color effects lies in the nanostructure and the resulting band structure. Next to the absence of states within the bandgap, there is another interesting feature in the LDOS: close to the bandgap, the LDOS is enhanced, the states missing within the bandgap are redistributed at the edges of the bandgap. Both these LDOS features, the absence of states within the bandgap as well as the enhancement close to the bandgap, have been employed for light-trapping in (silicon) solar cells.^{74–76} In the following, only examples using crystalline silicon as absorber material will be highlighted. The presented examples show that the absorption enhancement can be impressive at distinct wavelengths.^{25,42,70,74,75,77}

Yu et al. derived a fundamental limit of nanophotonic light trapping in solar cells by analytically determining the number of modes, that is, LDOS, that results from sub- and near-wavelength periodic structures.^{70,77} They found an enhancement of around $12n^2$ to be possible, however, at a narrow periodicity size to wavelength ratio.⁷⁰ Mokkapati and Catchpole summarized the limits of nanophotonic light trapping in their 2012 review paper and also point out that enhancements beyond the Lambertian limit in bulk structures must have a limited acceptance angle due to étendue conservation.³⁸ Bermel et al. and Zeng et al. compare photonic crystals of one, two, and three dimensions with metals for application as a rear reflector in solar cells.^{74,78} Devashish et al. computationally showed absorption enhancement within thin silicon through a combination of diffraction into guided modes and LDOS enhancement close to the photonic bandgap.⁷⁵ A recent perspective by Garnett et al. showcases gratings for various PV applications.⁷⁹

A popular class of two-dimensional photonic crystals are periodic nanowire and microwire arrays.^{80–84} As one example, Garnett and Yang reported a factor 73 of path length enhancement.⁸¹ The inverse geometry, nanohole arrays, has also been explored for light-trapping silicon solar cells.⁸⁵ While the cited literature shows promising absorption enhancements, the high surface area inherent to nanostructures can lead to high surface recombination⁸¹ as explained at the end of

this paper. Nevertheless, some groups have achieved good solar cell characteristics with silicon microwires.^{86,87} As one example, Kim et al. report 16.92% efficiency with 1.57-μm-thick microwires.⁸⁶ It should be noted that such nanowire/microwire and hole arrays are not always periodic.

5.3 | Nonperiodic nanostructures

In this chapter, we will discuss light-trapping strategies based on non-periodic structures with structure size similar to the light wavelengths involved. Above, we saw for the ray optical regime that random pyramids outperform periodic structures as the random nature enables to access all states within the silicon and hence approaches the properties of a Lambertian reflector.^{54,55} Further, we saw that periodic nanostructures provide great enhancement but are limited to narrow wavelength regimes. This poses the question whether nonperiodic nanostructures could provide a solution for broadband absorption enhancement.

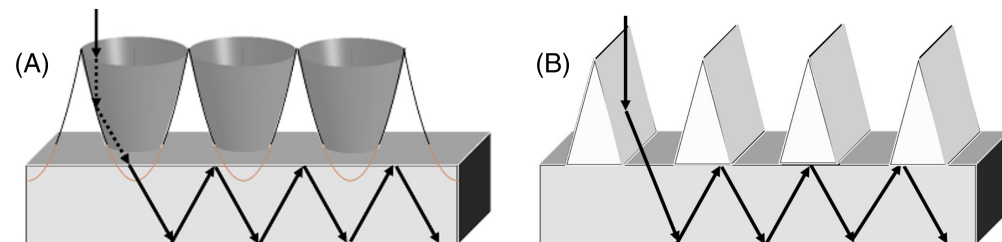
To this end, promising results were obtained through modulated surfaces with random features at different length scales, including nanocones and micropyramids.^{88,89} What is to date the record absorption within 1-μm-thick crystalline silicon and would correspond to an equivalent short-circuit density of 26.3 mA/cm² was achieved with a hyperuniform texture.⁹⁰

A further approach to achieve enhanced absorption with non-periodic nanostructures is the creation of a Fabry-Pérot cavity with the absorber material lying within this cavity and either metals or dielectric thin films effectively acting as mirrors.^{91,92} This approach is based on the principle of multi-beam interference and therefore has inherently narrow wavelength response.⁹³ For silicon solar cells, such an approach would only work for a narrow wavelength regime or in combination with spectrum splitting optics.⁹²

5.4 | Mesoscopic and macroscopic external light-trapping structures, and angle restriction

Another approach to achieve light trapping in silicon solar cells is the use of reflective external light-trapping structures with length scales larger than the involved wavelengths. Such structures can be modeled employing geometrical optics. The two most prominent designs are concentrators with parabolic cross-sectional (Figure 9A)^{47,94,95} and triangular cross-sectional lines (Figure 9B)^{40,96–98}.

FIGURE 9 Schematics of (A) 3D-printed concentrator arrays for external light trapping⁹⁴ and (B) effectively transparent contacts (ETCs) for light trapping^{40,96–98} [Colour figure can be viewed at wileyonlinelibrary.com]



Contrary to all approaches that feature structures with dimension on the same scale as the involved wavelength, larger structure sizes can achieve nearly uniform broadband response. Wavelength dependence is solely caused by the wavelength-dependent absorption and reflection properties of the metal structures. However, the optical properties depend on the angle of the incident light. As explained in Section 4.3, the better the trapping performance, the smaller the acceptance angle of the structure.^{41,97} A small acceptance angle means that sun tracking would be required and that diffused light cannot be converted efficiently.

5.5 | Plasmonic effects for solar cells

A literal gold rush in nanophotonics research set on in the early 2000s with the nascent of plasmonics.⁹⁹ In 2011, Atwater and Polman published what is to date one of—if not even—the most cited paper in field of light management for PVs: Plasmonics for improved photovoltaic devices.¹⁰⁰ Plasmonic solar cells promised to achieve improved light trapping through two main mechanisms: light scattering and near-field concentration of light.^{100,101} Surface plasmons occur at the interface of metals and dielectrics and are collective oscillations of the free electron gas inside the metal and the electromagnetic wave inside the dielectric.^{69,99,102} For decreasing wavelengths, the group velocity of surface plasmons decreases leading to strong localization—a property that has opened up new opportunities for sensing^{103–105} and microscopy.^{106–108} Enrichi et al. provide a comprehensive overview on plasmonic-enhanced solar cells in their 2018 review.¹⁰⁹ In recent years, efforts to use plasmonics in PV devices have lost momentum due to the significant optical losses inherent to plasmonic structures.¹⁰⁹ Instead, the focus has shifted to dielectric nanostructures, which can achieve similar scattering properties with less parasitic absorption. Such structures were already introduced in Sections 5.2 and 5.3. In the following, the advantages and disadvantages of different materials and textures will be discussed with regard to losses through parasitic absorption and surface recombination.

6 | PARASITIC ABSORPTION AND SURFACE RECOMBINATION

When assessing the absorption enhancement of light-trapping strategies, it needs to be carefully distinguished between absorption within the silicon and absorption occurring in other involved materials, so-called parasitic absorption. In most cases, the parasitically absorbed light does not contribute to the photocurrent.²⁷ Parasitic absorption is particularly pronounced in plasmonic systems. The strong localization of electromagnetic fields within the metal leads to strong absorption, which ultimately dissipates as Joule heat.¹¹⁰ Similarly, also the field enhancement in dielectric nanostructures leads to parasitic absorption. Through careful material design, making very clean crystals that do not have any resonances in the desired frequency range, it is possible to create low-loss dielectric nanostructures. Nevertheless,

parasitic absorption should always be carefully determined computationally and/or in experiments when reporting on absorption enhancement.

An elegant way to avoid parasitic absorption through field enhancement in scattering structures is the texturing of the absorbing silicon itself. In this case, the light absorption occurs primarily within the silicon. The downside of this approach is that it automatically increases the surface area of the crystalline silicon and thereby also the surface recombination. The best performing silicon solar cells rely on low surface recombination ensured by surface passivation. The resulting charge carrier lifetime of several milliseconds allows for record open-circuit voltage of 750 mV.³² But even with the best passivation strategies, increasing the surface area will always lead to increased surface recombination. Furthermore, electromagnetic field enhancement and therefore increased absorption primarily occurs in sharp and small features, which naturally are close to a surface, enhancing the performance losses from surface recombination.

In summary, for a real silicon solar cell, there is a trade-off between parasitic absorption, resulting from photonic support structures made of a material other than the crystalline silicon absorber layer, and surface recombination, resulting from texturing the crystalline silicon and thereby increasing surface area. Both these detrimental effects should be carefully considered when designing new light-trapping strategies.

7 | CONCLUSION

This review paper provides an overview of the physics involved in light trapping in solar cells with special focus on crystalline silicon. The Lambertian ($4n^2$) limit was derived, and it was explained how this limit can only be overcome through modification of the LDOS within the absorber or within the surrounding air. The reduction of LDOS within the surrounding air is equivalent with angle restriction³⁸ and therefore cannot work properly without sun tracking or under diffused conditions.

Section 5 presents examples of how the Lambertian limit can be approached using different scattering surfaces, most prominently, pyramidal textures. Furthermore, strategies for LDOS enhancements within the silicon (e.g., photonic crystals) and LDOS reduction within the surrounding air (e.g., angle restriction with external macroscopic and mesoscopic optics) were presented.

When choosing a certain light-trapping approach for a solar cell, several aspects should be taken into account such as the thickness of the cell, the bandwidth of the light that needs to be trapped, and the angle under which light needs to be accepted. For solar cells thicker than several micrometers, random pyramids provide close to ideal randomization of light and approach the Lambertian limit. Without constraining the acceptance angle or bandwidth of the trapped light, improvements are not possible. If the thickness of the absorber is reduced to several micrometers, random pyramids are no longer viable as Lambertian scatterers. Structures that employ smaller features or that are situated external to the absorber need to be considered.

It is important to distinguish between absorption enhancement within the silicon absorber layer and absorption within other components, also known as parasitic absorption. Parasitic absorption usually does not contribute to the photocurrent and is instead dissipated into heat. This loss mechanism is particularly pronounced in structures in which considerable electromagnetic field enhancement occurs within materials other than the crystalline silicon such as it is the case in plasmonic structures. Researchers working on light-trapping strategies should carefully evaluate their results with respect to parasitic absorption and angle acceptance. If absorption enhancement beyond the Lambertian limit is observed, the structure needs to provide either LDOS enhancement within the absorber or LDOS reduction (and thereby, acceptance angle reduction) outside the absorber. If none of these conditions are present, then absorption enhancement beyond the Lambertian limit is with today's knowledge not possible.

ORCID

Rebecca Saive  <https://orcid.org/0000-0001-7420-9155>

REFERENCES

1. Yablonovitch E. Statistical ray optics. *JOSA*. 1982;72(7):899-907.
2. Green MA. Silicon photovoltaic modules: a brief history of the first 50 years. *Prog Photovolt Res Appl*. 2005;13(5):447-455.
3. Fraunhofer Institute for Solar Energy Systems. Photovoltaics report. <https://www.ise.fraunhofer.de/content/dam/ise/de/documents/publications/studies/Photovoltaics-Report.pdf>. 2020.
4. Chapin DM, Fuller C, Pearson G. A new silicon *p-n* junction photocell for converting solar radiation into electrical power. *J Appl Phys*. 1954;25(5):676-677.
5. Lide DR. *CRC Handbook of Chemistry and Physics*. Boca Raton, FL: CRC Press; 2004.
6. Bye G, Ceccaroli B. Solar grade silicon: technology status and industrial trends. *Sol Energy Mater Sol Cells*. 2014;130:634-646.
7. Woodhouse MA, Smith B, Ramdas A, Margolis RM. Crystalline silicon photovoltaic module manufacturing costs and sustainable pricing: 1H 2018 Benchmark and Cost Reduction Road Map. National Renewable Energy Lab. (NREL), Golden, CO, USA. 2019.
8. Louwen A, Van Sark W, Schropp R, Faaij A. A cost roadmap for silicon heterojunction solar cells. *Sol Energy Mater Sol Cells*. 2016;147:295-314.
9. Green MA. Self-consistent optical parameters of intrinsic silicon at 300 K including temperature coefficients. *Sol Energy Mater Sol Cells*. 2008;92(11):1305-1310.
10. Fonash S. *Introduction to Light Trapping in Solar Cell and Photo-Detector Devices*. London, UK: Elsevier; 2014.
11. Bludau W, Onton A, Heinke W. Temperature dependence of the band gap of silicon. *J Appl Phys*. 1974;45(4):1846-1848.
12. Chelikowsky JR, Cohen ML. Electronic structure of silicon. *Phys Rev B*. 1974;10(12):5095-5107.
13. Sze SM, Ng KK. *Physics of Semiconductor Devices*. Hoboken, New Jersey: John Wiley & Sons, Inc.; 2006.
14. Aspnes DE, Studna A. Dielectric functions and optical parameters of Si, Ge, GaP, GaAs, GaSb, InP, InAs, and InSb from 1.5 to 6.0 eV. *Phys Rev B*. 1983;27(2):985-1009.
15. Chen H-L, Cattoni A, De Lépinay R, et al. A 19.9%-efficient ultrathin solar cell based on a 205-nm-thick GaAs absorber and a silver nanostructured back mirror. *Nat Energy*. 2019;4(9):761-767.
16. Honsberg CB. Silicon solar cell parameters. <https://www.pveducation.org/>. 2020.
17. Honsberg CB. Module materials. <https://www.pveducation.org/>. 2020.
18. Wang S, Weil BD, Li Y, et al. Large-area free-standing ultrathin single-crystal silicon as processable materials. *Nano Lett*. 2013;13(9):4393-4398.
19. Blakers A, Armour T. Flexible silicon solar cells. *Sol Energy Mater Sol Cells*. 2009;93(8):1440-1443.
20. Cui Y. Flipping thin silicon. <https://www.youtube.com/watch?v=e71Z0Kt3bsQ>. 2014.
21. Cui Y. Cutting thin silicon. <https://www.youtube.com/watch?v=PFyKfkwPRfs>. 2014.
22. Kayes BM, Zhang L, Twist R, Ding I-K, Higashi GS. Flexible thin-film tandem solar cells with >30% efficiency. *IEEE J Photovolt*. 2014;4(2):729-733.
23. Kayes BM Nie H, Twist R, Spruytte SG, Reinhardt F, Kizilyalli IC, Higashi GS. 27.6% conversion efficiency, a new record for single-junction solar cells under 1 sun illumination, in 2011 37th IEEE Photovoltaic Specialists Conference. IEEE; 2011:4-8.
24. Gaucher A, Cattoni A, Dupuis C, et al. Ultrathin epitaxial silicon solar cells with inverted nanop pyramid arrays for efficient light trapping. *Nano Lett*. 2016;16(9):5358-5364.
25. Xue M, Nazif KN, Lyu Z, et al. Free-standing 2.7 μm thick ultrathin crystalline silicon solar cell with efficiency above 12.0%. *Nano Energy*. 2020;70:104709.
26. Zhao J, Wang A, Altermatt PP, Wenham SR, Green MA. 24% efficient silicon solar cells. In: *Proceedings of 1994 IEEE 1st World Conference on Photovoltaic Energy Conversion—WCPEC (A Joint Conference of PVSC, PVSEC and PSEC)*. Vol.2. Waikoloa, HI, USA: IEEE; 1994: 1477-1480.
27. Holman ZC, Descoedres A, Barraud L, et al. Current losses at the front of silicon heterojunction solar cells. *IEEE J Photovolt*. 2012;2(1):7-15.
28. Honsberg CB. Open-circuit voltage. <https://www.pveducation.org/>. 2021.
29. Würfel P, Würfel U. *Physics of Solar Cells: From Basic Principles to Advanced Concepts*. Weinheim, Germany: Wiley-VCH Verlag GmbH & Co. KGaA; 2016.
30. Augusto AFR, Karas J, Balaji P, Bowden S, King RR. Exploring the practical efficiency limit of silicon solar cells using thin solar-grade substrates. *J Mater Chem A*. 2020;8(32):16599-16608.
31. Balaji P, Dauksher WJ, Bowden SG, Augusto A. Improving surface passivation on very thin substrates for high efficiency silicon heterojunction solar cells. *Sol Energy Mater Sol Cells*. 2020; 216:110715.
32. Herasimenka SY, Dauksher WJ, Bowden SG. >750mV open circuit voltage measured on 50 μm thick silicon heterojunction solar cell. *Appl Phys Lett*. 2013;103(5):053511.
33. Sai H, Umishio H, Matsui T, et al. Impact of silicon wafer thickness on photovoltaic performance of crystalline silicon heterojunction solar cells. *Jpn J Appl Phys*. 2018;57(8S3):08RB10.
34. Sinton RA, Cuevas A. Contactless determination of current-voltage characteristics and minority-carrier lifetimes in semiconductors from quasi-steady-state photoconductance data. *Appl Phys Lett*. 1996; 69(17):2510-2512.
35. Sinton R, Cuevas A. A quasi-steady-state open-circuit voltage method for solar cell characterization, in *Proceedings of the 16th European Photovoltaic Solar Energy Conference*, 2000;1152.
36. Green MA. Solar cell fill factors: general graph and empirical expressions. *SSEle*. 1981;24(8):788-789.
37. Jain A, Kapoor A. Exact analytical solutions of the parameters of real solar cells using Lambert W-function. *Sol Energy Mater Sol Cells*. 2004;81(2):269-277.
38. Mokkapati S, Catchpole K. Nanophotonic light trapping in solar cells. *J Appl Phys*. 2012;112(10):101101.

39. Green MA. Lambertian light trapping in textured solar cells and light-emitting diodes: analytical solutions. *Prog Photovolt Res Appl.* 2002; 10(4):235-241.
40. Saive R, Russell TC, Atwater HA. Enhancing the power output of bifacial solar modules by applying effectively transparent contacts (ETCs) with light trapping. *IEEE J Photovolt.* 2018;8(5): 1183-1189.
41. Rau U, Paetzold UW, Kirchartz T. Thermodynamics of light management in photovoltaic devices. *Phys Rev B.* 2014;90(3):035211.
42. Tobias I, Luque A, Marti A. Light intensity enhancement by diffracting structures in solar cells. *J Appl Phys.* 2008;104(3):034502.
43. Welford WT, Winston R. *Optics of Nonimaging Concentrators. Light and Solar Energy.* 1978.
44. Pal S, Reinders A, Saive R. Simulation of bifacial and monofacial silicon solar cell short-circuit current density under measured spectro-angular solar irradiance. *IEEE J Photovolt.* 2020;10(6):1803-1815.
45. Bittkau K, Nadi SA, Ding K, Rau U. Geometrical light trapping in thin c-Si solar cells beyond Lambertian limit, in 2019 IEEE 46th Photovoltaic Specialists Conference (PVSC), 2019;799-802: IEEE.
46. Shockley W, Queisser HJ. Detailed balance limit of efficiency of p-n junction solar cells. *J Appl Phys.* 1961;32(3):510-519.
47. Kosten ED, Newman BK, Lloyd JV, Polman A, Atwater HA. Limiting light escape angle in silicon photovoltaics: ideal and realistic cells. *IEEE J Photovolt.* 2014;5(1):61-69.
48. Kosten ED, Atwater JH, Parsons J, Polman A, Atwater HA. Highly efficient GaAs solar cells by limiting light emission angle. *Light: Sci Appl.* 2013;2(1):e45.
49. Bean KE. Anisotropic etching of silicon. *IEEE Trans Electron Dev.* 1978;25(10):1185-1193.
50. Campbell P, Green MA. Light trapping properties of pyramidal textured surfaces. *J Appl Phys.* 1987;62(1):243-249.
51. Russell TC, Saive R, Augusto A, Bowden SG, Atwater HA. The influence of spectral albedo on bifacial solar cells: a theoretical and experimental study. *IEEE J Photovolt.* 2017;7(6):1611-1618.
52. Baker-Finch SC, McIntosh KR. Reflection of normally incident light from silicon solar cells with pyramidal texture. *Prog Photovolt Res Appl.* 2011;19(4):406-416.
53. Guan L, Shen G, Liang Y, et al. Double-sided pyramid texturing design to reduce the light escape of ultrathin crystalline silicon solar cells. *Opt Laser Technol.* 2019;120:105700.
54. Manzoor S, Filipič M, Topič M, Holman Z. Revisiting light trapping in silicon solar cells with random pyramids, in 2016 IEEE 43rd Photovoltaic Specialists Conference (PVSC), 2016;2952-2954: IEEE.
55. Manzoor S, Filipič M, Onno A, Topič M, Holman ZC. Visualizing light trapping within textured silicon solar cells. *J Appl Phys.* 2020;127(6): 063104.
56. Razzaq A, Depauw V, Cho J, et al. Periodic inverse nanopyradim gratings for light management in silicon heterojunction devices and comparison with random pyramid texturing. *Sol Energy Mater Sol Cells.* 2020;206:110263.
57. Branham MS, Hsu WC, Yerci S, et al. Empirical comparison of random and periodic surface light-trapping structures for ultrathin silicon photovoltaics. *Advanced Optical Materials.* 2016;4(6):858-863.
58. Wang Y, Yang L, Liu Y, et al. Maskless inverted pyramid texturization of silicon. *Sci Rep.* 2015;5(1):1-6.
59. Zhao J, Wang A, Green MA. 24.5% Efficiency silicon PERT cells on MCZ substrates and 24.7% efficiency PERL cells on FZ substrates. *Prog Photovolt Res Appl.* 1999;7(6):471-474.
60. Campbell P, Green MA. High performance light trapping textures for monocrystalline silicon solar cells. *Sol Energy Mater Sol Cells.* 2001; 65(1-4):369-375.
61. Chu A, Wang J, Tsai Z, Lee C. A simple and cost-effective approach for fabricating pyramids on crystalline silicon wafers. *Sol Energy Mater Sol Cells.* 2009;93(8):1276-1280.
62. Han Y, Yu X, Wang D, Yang D. Formation of various pyramidal structures on monocrystalline silicon surface and their influence on the solar cells. *J Nanomater.* 2013;2013:716012.
63. Chen Q, Liu Y, Wang Y, et al. Optical properties of a random inverted pyramid textured silicon surface studied by the ray tracing method. *Sol Energy.* 2019;186:392-397.
64. Baker-Finch SC, McIntosh KR. Reflection distributions of textured monocrystalline silicon: implications for silicon solar cells. *Prog Photovolt Res Appl.* 2013;21(5):960-971.
65. McIntosh KR, Baker-Finch SC. OPAL 2: rapid optical simulation of silicon solar cells, in 2012 38th IEEE Photovoltaic Specialists Conference (PVSC), 2012; 000265-000271: IEEE.
66. Höhn O, Tucher N, Bläsi B. Theoretical study of pyramid sizes and scattering effects in silicon photovoltaic module stacks. *Opt Express.* 2018;26(6):A320-A330.
67. Yoshikawa K, Kawasaki H, Yoshida W, et al. Silicon heterojunction solar cell with interdigitated back contacts for a photoconversion efficiency over 26%. *Nat Energy.* 2017;2:17032.
68. Saive R, Borsuk AM, Emmer HS, et al. Effectively transparent front contacts for optoelectronic devices. *Adv Opt Mater.* 2016;4(10): 1470-1474.
69. Saleh BE, Teich MC. *Fundamentals of Photonics.* Hoboken, New Jersey: John Wiley & Sons, Inc.; 2019.
70. Yu Z, Raman A, Fan S. Fundamental limit of nanophotonic light trapping in solar cells. *Proc Natl Acad Sci.* 2010;107(41):17491-17496.
71. Wang KX, Yu Z, Liu V, Cui Y, Fan S. Absorption enhancement in ultrathin crystalline silicon solar cells with antireflection and light-trapping nanocone gratings. *Nano Lett.* 2012;12(3):1616-1619.
72. Lodahl P. All-solid-state quantum optics employing quantum dots in photonic crystals. In: *Quantum Optics with Semiconductor Nanostructures.* Elsevier; 2012:395-422e.
73. Yablonovitch E. Photonic crystals: semiconductors of light. *Sci Am.* 2001;285(6):46-55.
74. Bermel P, Luo C, Zeng L, Kimerling LC, Joannopoulos JD. Improving thin-film crystalline silicon solar cell efficiencies with photonic crystals. *Opt Express.* 2007;15(25):16986-17000.
75. Devashish D, Saive R, Van Der Vegt J, Vos WL. Absorption enhancement of a thin silicon film with a 3D photonic band gap crystal back reflector, in The European Conference on Lasers and Electro-Optics, 2019.
76. Mallick SB, Agrawal M, Peumans P. Optimal light trapping in ultrathin photonic crystal crystalline silicon solar cells. *Opt Express.* 2010; 18(6):5691-5706.
77. Yu Z, Raman A, Fan S. Fundamental limit of light trapping in grating structures. *Opt Express.* 2010;18(103):A366-A380.
78. Zeng L, Bermel P, Yi Y, et al. Demonstration of enhanced absorption in thin film Si solar cells with textured photonic crystal back reflector. *Appl Phys Lett.* 2008;93(22):221105.
79. Garnett EC, Ehrler B, Polman A, Alarcon-Llado E. Photonics for photovoltaics: advances and opportunities. *ACS Photonics.* 2021;8(1): 61-70.
80. Lin C, Povinelli ML. Optical absorption enhancement in silicon nanowire arrays with a large lattice constant for photovoltaic applications. *Opt Express.* 2009;17(22):19371-19381.
81. Garnett E, Yang P. Light trapping in silicon nanowire solar cells. *Nano Lett.* 2010;10(3):1082-1087.
82. Han SE, Chen G. Toward the Lambertian limit of light trapping in thin nanostructured silicon solar cells. *Nano Lett.* 2010;10(11): 4692-4696.
83. Warren EL, Atwater HA, Lewis NS. Silicon microwire arrays for solar energy-conversion applications. *J Phys Chem C.* 2014;118(2): 747-759.
84. Kelzenberg MD. *Silicon Microwire Photovoltaics.* Pasadena, CA, USA: California Institute of Technology; 2010.

85. Han SE, Chen G. Optical absorption enhancement in silicon nanohole arrays for solar photovoltaics. *Nano Lett.* 2010;10(3):1012-1015.
86. Kim H-S, Patel DB, Kim H, et al. Electrical and optical properties of Si microwire solar cells. *Sol Energy Mater Sol Cells.* 2017;164:7-12.
87. Um H-D, Lee K, Hwang I, et al. Progress in silicon microwire solar cells. *J Mater Chem A.* 2020;8(11):5395-5420.
88. Ingenito A, Isabella O, Zeman M. Nano-cones on micro-pyramids: modulated surface textures for maximal spectral response and high-efficiency solar cells. *Prog Photovolt Res Appl.* 2015;23(11):1649-1659.
89. Isabella O, Krč J, Zeman M. Modulated surface textures for enhanced light trapping in thin-film silicon solar cells. *Appl Phys Lett.* 2010;97(10):101106.
90. Tavakoli N, Spalding R, Koppejan P, Gkantzounis G, Wang C, Röhrich R, Kontoleta E, Koenderink AF, Sapienza R, Florescu M, Alarcon-Llado E. Over 65% sunlight absorption in a 1 μm Si slab with hyperuniform texture. <https://www.researchsquare.com/article/rs-69198/v1>. 2020.
91. Jariwala D, Davoyan AR, Tagliabue G, Sherrott MC, Wong J, Atwater HA. Near-unity absorption in van der Waals semiconductors for ultrathin optoelectronics. *Nano Lett.* 2016;16(9):5482-5487.
92. Durmaz Z, Husein S, Saive R. Thin silicon interference solar cells for targeted or broadband wavelength absorption enhancement. *Opt Express.* 2021;29(3):4324-4337.
93. Hecht E. *Optics*. 4thed. USA: Addison Wesley; 2002.
94. van Dijk L, Marcus EP, Oostra AJ, Schropp RE, Di Vece M. 3D-printed concentrator arrays for external light trapping on thin film solar cells. *Sol Energy Mater Sol Cells.* 2015;139:19-26.
95. Atwater J, Spinelli P, Kosten E, et al. Microphotonic parabolic light directors fabricated by two-photon lithography. *Appl Phys Lett.* 2011;99(15):151113.
96. Saive R, Atwater HA. Mesoscale trumps nanoscale: metallic mesoscale contact morphology for improved light trapping, optical absorption and grid conductance in silicon solar cells. *Opt Express.* 2018;26(6):A275-A282.
97. Saive R, Russell TC, Atwater HA. Light trapping in bifacial solar modules using effectively transparent contacts (ETCs), in 2018 IEEE 7th World Conference on Photovoltaic Energy Conversion (WCPEC) (A Joint Conference of 45th IEEE PVSC, 28th PVSEC & 34th EU PVSEC). IEEE; 2018:0045-0048.
98. Saive R, Augusto A, Bowden S, Atwater HA. Enhanced light trapping in thin silicon solar cells using effectively transparent contacts (ETCs) in 2017 IEEE 44th Photovoltaic Specialists Conference (PVSC), 2017: IEEE.
99. Maier SA, Brongersma ML, Kik PG, Meltzer S, Requicha AA, Atwater HA. Plasmonics—a route to nanoscale optical devices. *Adv Mater.* 2001;13(19):1501-1505.
100. Atwater HA, Polman A. Plasmonics for improved photovoltaic devices. In: *Materials for Sustainable Energy: A Collection of Peer-Reviewed Research and Review Articles from Nature Publishing Group*. World Scientific; 2011:1-11.
101. Catchpole KR, Polman A. Plasmonic solar cells. *Opt Express.* 2008;16(26):21793-21800.
102. Maier SA. *Plasmonics: Fundamentals and Applications*. New York, USA: Springer Science+Business Media LLC; 2007.
103. Li M, Cushing SK, Wu N. Plasmon-enhanced optical sensors: a review. *Analyst.* 2015;140(2):386-406.
104. Chen Y, Ming H. Review of surface plasmon resonance and localized surface plasmon resonance sensor. *Photonic Sens.* 2012;2(1):37-49.
105. Sharma AK, Jha R, Gupta B. Fiber-optic sensors based on surface plasmon resonance: a comprehensive review. *IEEE Sensors J.* 2007;7(8):1118-1129.
106. Bocková M, Slabý J, Špringer T, Homola J. Advances in surface plasmon resonance imaging and microscopy and their biological applications. *Annu Rev Anal Chem.* 2019;12(1):151-176.
107. Wong CL, Olivo M. Surface plasmon resonance imaging sensors: a review. *Plasmonics.* 2014;9(4):809-824.
108. Rothenhäusler B, Knoll W. Surface-plasmon microscopy. *Nature.* 1988;332(6165):615-617.
109. Enrichi F, Quandt A, Righini GC. Plasmonic enhanced solar cells: summary of possible strategies and recent results. *Renew Sustain Energy Rev.* 2018;82:2433-2439.
110. Sambles J, Innes R. A comment on nonlinear optics using surface plasmon-polaritons. *J Mod Opt.* 1988;35(5):791-797.

How to cite this article: Saive R. Light trapping in thin silicon solar cells: A review on fundamentals and technologies. *Prog Photovolt Res Appl.* 2021;29(10):1125-1137. <https://doi.org/10.1002/pip.3440>